Antihormonal potential of selected D-homo and D-seco estratriene derivatives

Suzana S. Jovanović-Šanta [a,*], Edward T. Petri [b], Olivera R. Klisurić [c], Mihály Szécsi [d], Radmila Kovačević [b], Julijana A. Petrović [a]

[a] Department of Chemistry, Biochemistry and Environmental Protection, Faculty of Science, University of Novi Sad, Trg Dositeja Obradovića 3, 21000 Novi Sad, Serbia
[b] Department of Biology and Ecology, Faculty of Science, University of Novi Sad, Trg Dositeja Obradovića 2, 21000 Novi Sad, Serbia
[c] Department of Physics, Faculty of Science, University of Novi Sad, Trg Dositeja Obradovića 4, 21000 Novi Sad, Serbia
[d] First Department of Medicine, University of Szeged, Korányi fasor 8-10, H-6720 Szeged, Hungary

ARTICLE INFO

ABSTRACT

Since many estrogen derivatives exhibit anti-hormone or enzyme inhibition potential, a large number of steroidal derivatives have been synthesised from appropriate precursors, in order to obtain potential therapeutics for the treatment of hormone-dependent cancers. In molecular docking studies, based on X-ray crystallographic analysis, selected D-homo and D-seco estratriene derivatives were predicted to bind strongly to estrogen receptor α (ERα), aromatase and 17,20 lyase, suggesting they could be good starting compounds for antihormonal studies. Test results *in vivo* suggest that these compounds do not possess estrogenic activity, while some of them showed weak anti-estrogenic properties. *In vitro* anti-aromatase and anti-lyase assays showed partial inhibition of these two enzymes, while some compounds activated aromatase. Aromatase activators are capable of promoting estrogen synthesis for treatment of pathological conditions caused by estrogen depletion, *e.g.* osteopenia or osteoporosis.

1. Introduction

Steroid hormones regulate many different physiological processes in humans, through all phases of life. Tissue-specific enzymes catalyze steroidogenesis, which starts with initial entry of cytosolic cholesterol into the mitochondrion, and then proceeds with conversion of cholesterol to the biologically active androgen, followed by estrogen hormones. Enzymes belonging to cytochrome P450 enzymes and hydroxysteroid dehydrogenases catalyze adrenal, ovarian, testicular, placental and other steroidogenic processes [1].

The reduction of circulating steroid hormones and/or blockade of steroid action in cancer tissues are still primary goals in the current strategy for breast- and prostate-cancer treatment [2]. In the treatment of androgen-dependent tumors, antiandrogens, as well as 17α-hydroxylase/C17,20 lyase (CYP17A1) and 5α-reductase inhibitors are the most promising therapeutics [2,3].

Since estrogen hormones are involved in the development and growth of breast tumors, estrogen deprivation remains a key therapeutic approach. Endocrine agents are designed to inhibit the production of estrogen or to block its action at the estrogen receptor [2,4]. For many years, tamoxifen, an antiestrogen that compete with estradiol for estrogen receptor, was the most important therapeutic in the hormonal therapy for all stages of postmenopausal patients with estrogen-receptor–positive cancers. However, tamoxifen does not completely prevent the action of endogenous estrogen, and this remaining partial estrogen agonist activity is probably responsible for some of its undesirable side effects, such as an increased risk of endometrial cancer.

On the other hand, the enzyme aromatase [5], which catalyzes the key and final step of estrogen synthesis, namely conversion of C19 steroids to estrogens, acts as a master switch in physiological and pathological processes. Apart from the fact that, unlike tamoxifen, aromatase inhibitors (AI) have no partial agonist activity, cancer cells could become resistant to this kind of therapy [6].

Thus, by combining these two breast cancer therapy approaches, the greatest benefit for patients can be realized [2,7–10].

Considering the partial agonistic effects of tamoxifen and the existence of breast cancer cells resistant to aromatase inhibitors, an important objective of researchers is to find new efficient strategies and/or more effective therapeutics for treating patients suffering from estrogen-dependent breast cancer, with no side effects or resistance.

* Corresponding author. Tel.: +381 21 485 2771; fax: +381 21 455 662.
  E-mail addresses: suzana.jovanovic-santa@dh.uns.ac.rs, santas021@gmail.com
(S.S. Jovanović-Šanta).

A broader project, directed towards preparation of potential antihormones and steroidogenesis enzymes inhibitors resulted in the synthesis of many D-modified steroidal compounds possessing promising antihormonal properties [11–18] Among others, 3-benzyloxy-17-hydroxy-16,17-secoestra-1,3,5(10)-trien-16-nitrile, was of special interest, as well as its corresponding 3-hydroxy derivative. Specifically, this compound showed practically complete loss of estrogenic activity, while displaying satisfactory antihormonal properties. On the other hand, its 3-hydroxy equivalent showed less antiestrogenic activity, with complete loss of estrogenic potency [11]. These facts prompted us to further pursue chemical transformations of this secocyanoalcohol, in order to study the influence of different modifications of the D-ring on the biological potential of new compounds.

2. Experimental

2.1. Synthesis and characterization of the newly synthesised compounds

2.1.1. General

Melting points were determined in open capillary tubes on a Büchi SMP apparatus and values are reported uncorrected. Infrared spectra (v in cm^{-1}) were recorded in KBr pellets on a Perkin-Elmer M457 or Carl Zeiss Specord 75 spectrophotometer. NMR-spectra were taken on a Bruker AC 250E spectrometer operating at 250 Hz (proton) and 62.9 Hz (carbon), using standard Bruker software. The signals are reported in ppm downfield from a tetramethylsylane internal standard (δ 0.00); symbols s, d, dd and m denote singlet, doublet, double doublet and multiplet, respectively. Mass spectra were recorded on a Finnigan-Math 8230 instrument, using chemical ionization (iso-butane) techniques; the first number denotes m/z value, and the ion abundances are given in parentheses.

2.1.2. 3-Benzyloxy-17-oxa-D-homo-estra-1,3,5(10)-triene-16-on (2)

Secocianoalcohol 1 (1 g, 2.67 mmol) was dissolved in benzene (5 mL) and p-toluenesulfonic acid (0.64 g, 3.37 mmol) was added. The reaction mixture was refluxed for 4 h. The catalyst was filtered off and the solvent was evaporated to dryness. The crude 3-benzyloxy-D-homo derivative 2 (0.96 g, 95.71%) was purified by column chromatography on silica gel (100 g, toluene-ethyl acetate /2:1/), giving 0.55 g (57.30%) of analytically pure 3-benzyloxy-17-oxa-D-homo-estra-1,3,5(10)-triene-16-on (2, mp. 162 °C).

IR spectrum: 3060, 2980–2960, 1750, 1620, 1250, 1050, 760, 740, 705

^{1}H NMR spectrum (CDCl$_3$): 1.05 (s, 3H, CH$_3$, C$_{18}$); 2.22 (2d, 3H, 1H$_{15}$ and 2 protons from the skeleton; J_{gem} = 18.61 Hz, $J_{15a,14}$ = 12.79 Hz); 2.85 (m, 3H, 1H$_{15}$ 2 protons from the skeleton); 3.98 (d, 1H, H$_{17a}$, J_{gem} = 10.69 Hz); 4.05 (d, 1H, H$_{17a}$); 5.05 (s, 2H, O-CH$_2$-C$_6$H$_5$); 6.74–7.47 (group of signals, 8H, aromatic protons).

^{13}C NMR-spectrum (CDCl$_3$): 14.98 (CH$_3$, C$_{18}$); 69.80 (O-CH$_2$-C$_6$H$_5$); 81.07 (C$_{17a}$); 156.87 (C$_3$); 170.64 (C=O).

Mass spectrum: 378 (9; (M + 2)$^+$); 377 (30; (M + 1)$^+$); 92 (19; (C$_7$H$_8$)$^+$); 91 (100; (C$_7$H$_7$)$^+$).

Anal. Calcd. for C$_{25}$H$_{28}$O$_3$: C, 79.78; H, 7.45. Found: C, 80.03; H, 7.64.

2.1.3. 3-Benzyloxy-16,17-secoestra-1,3,5(10)-triene-16,17-diol (3)

Compound 2 (0.52 g, 1.38 mmol) was dissolved under heating in a mixture of methanol and dichloromethane (2:1, 30 mL). To the cooled solution NaBH$_4$ (0.42 g, 11 mmol) was added stepwise. The reaction mixture was stirred for 20 min at room temperature and then refluxed for 40 min. After cooling, the resulting solution was acidified with dilute HCl (1:4) to pH 5. The obtained suspension

was extracted with dichloromethane (3 × 30 mL), collected extracts were washed with water, dried over anhydrous sodium sulfate and evaporated to dryness. The crude 3-benzyloxy D-secodiol 3 (0.43 g, 81.13%) was purified by column chromatography on silica gel (50 g, toluene-ethyl acetate /2:1/), giving 0.32 g (74.42%) of 3-benzyloxy-16,17-secoestra-1,3,5(10)-triene-16,17-diol (3) in form of a pale yellow oil, which after crystallization from the mixture dichloromethane-n-hexane gave white crystals of 3 (mp. 141 °C).

IR spectrum: 3500–3300, 2980–2900, 1630, 1515, 1300, 1270, 1050

^{1}H NMR spectrum (CDCl$_3$): 0.71 (s, 3H, CH$_3$, C$_{18}$); 2.87 (d, 2H, H$_{15}$, J_{gem} = 3.72 Hz); 3.10 (d, 1H, H$_{17a}$, J_{gem} = 11.78 Hz); 3.48 (s, 2H, HO–C$_{17}$ and HO–C$_{16}$); 3.59 (m, 1H, H$_{17b}$); 3.70 (d, 1H, H$_{16a}$, J_{gem} = 11.77 Hz); 3.91 (m, 1H, H$_{16b}$); 5.04 (s, 2H, O-CH$_2$-C$_6$H$_5$); 6.47–6.72 (group of signals, 8H, aromatic protons).

^{13}C NMR-spectrum (CDCl$_3$): 15.92 (CH$_3$, C$_{18}$); 30.52 (C$_{15}$); 64.04 (C$_{16}$); 69.90 (O-CH$_2$-C$_6$H$_5$); 70.01 (C$_{17}$); 156.67 (C$_3$).

Mass spectrum: 380 (20; M$^+$); 147 (37); 91 (100; (C$_7$H$_7$)$^+$).

Anal. Calcd. for C$_{25}$H$_{32}$O$_3$: C, 78.90; H, 8.47. Found: C, 79.24; H, 8.14.

2.1.4. 3-Hydroxy-17-oxa-D-homo-estra-1,3,5(10)-triene-16-on (4) and 16,17-secoestra-1,3,5(10)-triene-3,16,17-triol (5)

To the solutions of the appropriate 3-benzyloxy derivative (2, 0.30 g, 0.80 mmol, i.e. 3, 0.25 g, 0.67 mmol) in dichloromethane-methanol mixture (1:1, 3 mL), 10% Pd/C (0.15 g) was added. The suspensions were stirred at room temperature for 5, i.e. 3 h under an atmosphere of hydrogen. After removal of catalyst, the reaction mixtures were evaporated to dryness, yielding 0.22 g (95.65%), i.e. 0.11 g (56.60%) of crude 3-hydroxy-derivatives 4, i.e. 5. The crude product 4 was purified by column chromatography on silica gel (40 g, toluene-ethyl acetate /2:1/), whereby 0.18 g (81.81%) of analytically pure 3-hydroxy-17-oxa-D-homo-estra-1,3,5(10)-triene-16-on (4, mp. 205 °C) was obtained. On the other hand, flash chromatography of crude 5 on silica gel (n-hexane–acetone /3:2/), yielded 0.08 g (41.88%) of 16,17-secoestra-1,3,5(10)-triene-3,16,17-triol (5, mp. 201 °C) in form of colorless crystals.

2.1.5. Compound 4

IR spectrum: 3500–3300, 2970, 1730, 1300, 1270, 1050

^{1}H NMR spectrum (DMSO-d6): 0.92 (s, 3H, CH3, C18); 2.20 (m, 4H, 1H$_{15}$ and 3 protons from the skeleton); 2.72 (m, 3H, 1H$_{15}$ and 2 protons from the skeleton); 3.95 (2d, 2H, H$_{17a}$); 6.45 (d, 1H, H-4, $J_{4,2}$ = 2.58 Hz); 6.53 (dd, 1H, H-2, $J_{2,1}$ = 8.36 Hz, $J_{2,4}$ = 2.59 Hz); 7.06 (d, 1H, H-1, $J_{1,2}$ = 8.48 Hz); 9.03 (s, 1H, HO=C$_3$).

^{13}C NMR-spectrum (DMSO-d$_6$): 14.61 (CH$_3$, C$_{18}$); 80.15 (C$_{17a}$); 155.04 (C$_3$); 170.11 (C=O).

Mass spectrum: 288 (21; (M + 2)$^+$); 287 (44; (M + 1)$^+$); 286 (100; M$^+$); 259 (16); 172 (67); 159 (23); 145 (21); 133 (18); 107 (16).

Anal. Calcd. for C$_{18}$H$_{22}$O$_3$: C, 75.49; H, 7.74. Found: C, 75.24; H, 7.56.

2.1.6. Compound 5

IR spectrum: 3500–3300, 2970, 1630, 1600, 1515, 1380, 1300, 1270, 1050.

^{1}H NMR spectrum (DMSO-d$_6$): 0.65 (s, 3H, CH$_3$, C$_{18}$); 3.02 (dd, 1H, C$_{17a}$, J_{gem} = 11.0 Hz, $J_{H,OH}$ = 6.51 Hz); 3.32 (m, 2H, 1H$_{16}$ and 1H$_{17}$); 3.45 (m, 1H, H$_{16b}$); 4.47 (t, 1H, HO=C$_{17}$, J = 6.21 Hz); 4.72 (t, 1H, HO=C$_{16}$, J = 4.78 Hz); 6.42 (d, 1H, H-4, $J_{4,2}$ = 2.51 Hz); 6.50 (dd, 1H, H-2, $J_{2,1}$ = 8.43 Hz, $J_{2,4}$ = 2.58 Hz); 7.05 (d, 1H, H-1, $J_{1,2}$ = 8.50 Hz); 9.00 (s, 1H, HO=C$_3$).

^{13}C NMR-spectrum (DMSO-d$_6$): 15.96 (CH$_3$, C$_{18}$); 29.99 (C$_{15}$); 62.20 (C$_{16}$); 69.24 (C$_{17}$); 154.88 (C$_3$).

Mass spectrum: 290 (37; M$^+$); 272 (15; (M-H$_2$O)$^+$); 243 (15); 227 (48); 159 (100); 133 (39).

Anal. Calcd. for C$_{18}$H$_{26}$O$_3$: C, 74.44; H, 9.03. Found: C, 74.26; H, 8.99.

2.2. X-ray analysis

A single crystal of compound **5** was selected and glued onto a glass fiber. X-ray diffraction data were collected on a STOE *IPDS* diffractometer. The crystal to detector distance was 80.0 mm and graphite monochromated MoKα ($\lambda = 0.71073$ Å) radiation was employed. Data were reduced using the Stoe X-RED data reduction program [19]. A numerical absorption-correction was applied, and data were corrected for Lorentz, polarization, and background effects. Space group determinations were based on analysis of the Laue class and systematically absent reflections. The structure was defined by direct methods [20]. The figures were drawn using ORTEP3 [21] and PLATON [22]. Refinements were based on F^2 values and done by full-matrix least-squares [23] with all non-H atoms anisotropic. The positions of all non H-atoms were located by direct methods. The positions of hydrogen atoms were found from inspection of difference Fourier maps. The final refinement included atomic positional and displacement parameters for all non-H atoms. The non-H atoms were refined anisotropically. At the final stage of the refinement, H atoms from CH$_3$ group were positioned geometrically (C–H = 0.96 Å) and refined using a riding model with fixed isotropic displacement parameters. All other calculations were performed using PARST [24] and PLATON [22], as implemented in the WINGX [21] system of programs. The crystal data and refinement parameters are summarized in Table 1.

2.3. Molecular docking studies

2.3.1. Protein (receptor) structural co-ordinate preparation

Three-dimensional structural co-ordinates for estrogen receptor α (ERα: PDB ID 1A52), androgen receptor (AR: PDB ID 2AMA), Aromatase (CYP19A1: PDB ID 3EQM; enzyme classification (EC) number 1.14.14.14) and 17,20-lyase/17α-hydroxylase (CYP17A1: PDB ID 3RUK; EC 1.14.99.9 and 4.1.2.30) were obtained from the protein data bank (http://www.rcsb.org). Co-ordinates for ligands and all water molecules were removed using a text editor. Nonpolar hydrogen atoms were merged and receptor co-ordinate files saved in PDBQT format for docking simulations using 'receptor.c' in VEGA ZZ 3.0.1 [25].

2.3.2. Ligand structural co-ordinate preparation

Based on the X-ray crystal structures of compounds **1a** [14] and **5**, 3D structural models of other compounds were created in AVO-GADRO 1.0.3 (http://avogadro.openmolecules.net/) [26]. Hydrogen atoms were added and ligand geometries were optimized (MMFF94 force field: 500 steps of conjugate gradient energy minimization followed by 500 steps of steepest descent energy minimization with a convergence setting of 10×10^{-7}) in the program AVOGADRO. Nonpolar hydrogen atoms were merged and Gasteiger partial charges partial charges were calculated using the script 'ligand.c' in VEGA ZZ 3.0.1 and the resulting ligand coordinate files were saved in PDBQT format.

2.3.3. Grid parameter file preparation

Grid maps were calculated using AutoGrid 4 [27] and Auto-DockTools, based on the coordinates of ligands present in the crystal structures. Grid maps were calculated with the default grid box size of 70 × 70 × 65 points and grid spacing of 0.375 Å. Molecular docking simulations were conducted against the active site of each receptor. Thus, grid boxes were centered over the coordinates of ligands present in the receptor crystal structures: estradiol for

ERα, testosterone for AR, androstenedione for Aromatase and abiraterone for 17,20-lyase/17α-hydroxylase. Maps were calculated for each atom type (including hydrogen bond donors, acceptors and aromatic atoms) in the ligand along with an electrostatic and desolvation map (using the default dielectric value of −0.1465).

2.3.4. Docking parameter file preparation

Initial ligand position, orientation and dihedral offset values were set as random (default). The number of torsional degrees of freedom (*i.e.* rotatable bonds) for each ligand was determined during the ligand preparation stage in AutoDockTools [27]. Molecular docking studies were conducted using the Larmarckian genetic algorithm and all default parameters. The maximum number of energy evaluations was set to 2,500,000 and the GA population size was 150; 10 hybrid GA-LS runs were performed. Results were visualized using the program PyMol (http://www.pymol.org/). Autodock and AutoGrid calculations were conducted remotely at the National Biomedical Computational Resource (http://nbcr-222.ucsd.edu/opal2) [28] using the program PyRx virtual screening tool [29]. All control docking simulations using ligands present in X-ray crystal structures of the proteins were able to reproduce the ligand–protein interaction geometries present in the respective crystal structures. Based on these control docking simulations, predicted binding energies ⩽−10.00 kcal/mol were considered to be indicative of strong binding.

2.4. Biological tests

All experiments were approved by the Local Ethical Committee of the University of Novi Sad or Szeged and were performed and conducted in accordance with the principles and procedures of the NIH Guide for Care and Use of Laboratory Animals.

Table 1
Experimental details: Crystallographic data and refinement parameters.

Crystal data	
Chemical formula	C$_{18}$H$_{26}$O$_3$
M_r	290.39
Crystal system, space group	Orthorhombic, $P2_12_12_1$
Temperature (K)	293
a, b, c (Å)	10.195 (5), 6.675 (5), 23.145 (5)
V (Å^3)	1575.1 (15)
Z	4
Radiation type	Mo Kα
μ (mm^{-1})	0.08
Crystal size (mm)	0.25 × 0.23 × 0.21
Data collection	
Diffractometer	STOE *IPDS* diffractometer
Absorption correction	Numerical Stoe, *X-RED*, Data Reduction for STADI4 and *IPDS*, Revision 1.08. Stoe & Cie, Darmstadt, 1996, Germany
T_{min}, T_{max}	0.787, 0.953
No. of measured, independent and observed [$I > 2\sigma(I)$] reflections	18329, 2515, 1491
R_{int}	0.056
Refinement	
$R[F^2 > 2\sigma(F^2)]$, $wR(F^2)$, S	0.027, 0.050, 0.78
No. of reflections	2515
No. of parameters	283
No. of restraints	0
H-atom treatment	H atoms treated by a mixture of independent and constrained refinement
$\Delta\rho_{max}$, $\Delta\rho_{min}$ (e Å^{-3})	0.09, −0.08
Absolute structure	Flack H D (1983), Acta Cryst. A39, 876–881
Flack parameter	1.0 (12)

2.4.1. Uterotrophic and antiuterotrophic assay

The estrogenic and antiestrogenic effects of compounds **2**–**5** and tamoxifen were tested on experimental animals, using the utero-trophic and antiuterotrophic methods [30,11].

Immature Wistar strain female rats (21–23 days old, raised under controlled environmental conditions – temperature 22±2 °C and 14 h light/10 h dark), with food and water *ad libitum*) were randomly divided into groups of six to eight animals each. The animals were treated by subcutaneous injection once a day for 3 days with 0.1 mL of a solution of the test compound in olive oil, either solely or in combination with estradiol benzoate (EB). The control group obtained the vehicle only. The total adminis-tered amount of tested compounds was 5 mg/kg of body weight (b.w.), whereas the EB dose was 30 µg/kg b.w. The animals were sacrificed on the fourth day. The uteri were removed, dissected free of adhering fat and blotted dry after expulsion of uterine fluid and the wet weights were recorded.

The differences of uteri weights of treated and control animals served for the calculation of the agonistic and antagonistic effects [31]. Percentage of agonistic and antagonistic activity in immature rat uterine weight assays were calculated from the ratio of values recorded in the treated and control animals, thus:

$$\% \text{ agonism} = (C - A) \times 100/(B - A)$$
$$\% \text{ antagonism} = (B - D) \times 100/(B - A)$$

where *A*, *B*, *C* and *D* are uterine wet weights, corrected for differ-ences in body weight, *i.e.* (mg/100 g body weight) for vehicle alone, EB, test compound alone, and test compound plus EB groups, respectively.

2.4.2. Anti-aromatase assay

Chemicals used: Antiestradiol serum No. 244, was kindly sup-plied by Dr. G. D. Niswender (Colorado State University, CO, USA). Pregnant Mares' Serum Gonadotrophin (PMSG) was obtained from the Veterinary Institute Subotica (Serbia), $[1,2,6,7-^3H(N)]$ estradiol was obtained from New England Nuclear (Belgium), NADPH, testosterone and aminoglutethimide (AG) were obtained from Sigma (St. Louis, MO). All other reagents were of analytical grade.

Animals, treatment and assay: Anti-aromatase activity of the synthesised compounds was tested according to the procedure described elsewhere [12]. In brief, in the final volume of 0.25 mL, the incubation mixture contained testosterone as substrate, 1 mM NADPH, 0.1 M phosphate buffer (pH 7.4), tested compound and 0.125 mL of denucleated ovarian fraction (0.33 mg of protein, prepared by known procedure [32]). Parallel incubations without tested compounds were also run as control samples. The desired concentration of tested compounds was prepared by evaporating the necessary amount of stock solution (in organic solvent) and dissolving it in 0.1 M phosphate buffer. Mixtures were incubated for 15 min at 37 °C in a shaking water bath in 95% O_2 – 5% CO_2 atmosphere. The enzyme reaction was initiated by adding denucle-ated ovarian fraction and terminated by placing the tubes in an ice-cold bath. The samples were stored at −20 °C until assayed for estradiol by RIA. Estradiol production in control and experi-mental samples were calculated after subtraction of the corre-sponding blanks. Namely, two sets of blanks were run in parallel with control and experimental samples: in the first set, testoster-one and tested compounds were omitted in order to determine residual levels of estradiol and possible endogenous estradiol production in denucleated ovarian fractions used in each experiment, while in the second set, homogenate was omitted in order to determine cross-reactivity of testosterone and tested compounds.

For an assessment of anti-aromatase activity of the synthesised compounds, the given compounds were added in two concentra-tions (10 µM and 50 µM) to the incubation mixture containing 500 nM of testosterone as substrate (saturated concentration; the estimated K_m for testosterone was 49.17 nM, and V_{max} 5.76 pmol/min × mg protein). Standard anti-aromatase inhibitor, aminoglut-etimide, was tested in concentration 0.1 µM.

Statistics: The statistical significance was evaluated by two-tailed non-parametric Mann–Whitney test.
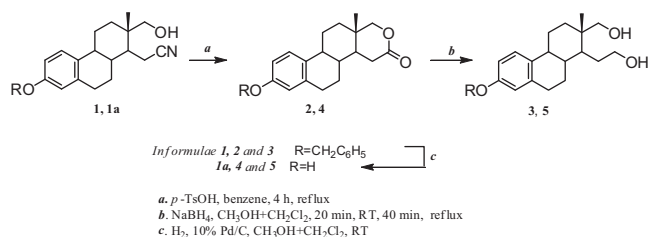
2.4.3. Anti-lyase assay

Chemicals used: Radioactive $[1,2,6,7-^3H]$17-hydroxyprogester-one was purchased from the American Radiolabeled Chemicals (St. Louis, MO, USA). Non-radioactive 17-hydroxyprogesterone and androst-4-ene-3, 17-dione standards, reference inhibitor keto-conazole and other chemicals and solvents with purity of analytical grade were purchased from Sigma (St. Louis, MO, USA). Kieselgel-G TLC layers (Si 254 F, 0.25 mm thick) were obtained from Merck (Darmstadt, Germany).

Inhibitory effects exerted on the $C_{17,20}$-lyase activity were determined by an *in vitro* radiosubstrate incubation method described in other publications [33,34]. In brief, adult Wistar rat testicular tissue was homogenized with an Ultra-Turrax in 0.1 M HEPES buffer (pH = 7.3) containing 1 mM EDTA and 1 mM dithio-treitol. Aliquots of this homogenate were incubated in 200 µL final volume at 37 °C for 20 min in the presence of 0.1 mM NADPH. 1 µM $[^3H]$17-hydroxyprogesterone (300000 dpm) was added to the incubate in 20 µL of a 25 v/v% propylene glycol solution. Test compounds were applied at 50 µM and introduced in 10 µL of DMSO. (These organic solvent contents did not reduce the enzyme activity substantially.) Control incubates without test substances, and incubates with the reference compound ketoconazole were also prepared in every series. Following incubation, the androst-4-ene-3,17-dione formed and the 17-hydroxyprogesterone remaining were isolated through extraction and a subsequent TLC separation on Kieselgel-G layers with the solvent system dichloromethane/diisopropyl ether/ethyl acetate (75:15:10 v/v). Ultraviolet light was used to trace the separated steroids. Spots were cut out and the radioactivity of the androst-4-ene-3,17-dione formed and the 17-hydroxyprogesterone remaining was measured by liquid scintillation counting (Packard Tri-Carb 2200CA). $C_{17,20}$-lyase activity was calculated from the radioactivity of the androst-4-ene-3,17-dione with correction of the recovery. Two experiments were performed with each test compound and mean enzyme activity results with standard deviations were determined.

3. Results and discussion

The starting compound, 3-benzyloxy-17-hydroxy-16,17-seco-estra-1,3,5(10)-trien-16-nitrile (**1**) was synthesised from estrone in several synthetic steps [11]. The syntheses of new compounds were performed according to Scheme 1. Namely, treatment of the starting secocyanoalcohol **1** with catalytic amounts of *p*-toluene-sulfonic acid in benzene afforded D-homoestratriene derivative **2**

a. *p*-TsOH, benzene, 4 h, reflux
b. NaBH₄, CH₃OH+CH₂Cl₂, 20 min, RT, 40 min, reflux
c. H₂, 10% Pd/C, CH₃OH+CH₂Cl₂, RT

Scheme 1. Synthesis of new D-homo and D-seco estratriene compounds.

in high yield, as a result of initial hydrolysis of nitrile function to carboxyl group, followed by successive cyclization. Treatment of D-homo derivative **2** with sodium borohydride in the mixture of solvents resulted in re-opening of D-ring, to give 16,17-seco-diol derivative **3**. Both of the newly-synthesised 3-benzyloxy derivatives **2** and **3** underwent hydrogenolysis at room temperature in the atmosphere of hydrogen, with Pd/C as catalyst, giving the appropriate 3-hydroxy D-homo (**4**) *i.e.* D-seco derivative (**5**) in satisfactory yields.

All the crude products were purified in similar fashion, by column chromatography on silica gel. Analytically pure compounds were then identified (based on IR, NMR and mass spectral data and elemental microanalyses) and used for biological tests.

The structure of 3-hydroxy-16,17-seco-diol **5** was confirmed by X-ray structural analysis. An ORTEP drawing of the molecular structure of compound **5** is depicted in Fig. 1.

Compound **5** crystallizes in orthorombic non-centrosymetric $P2_12_12_1$ space group with four molecules in the unit cell. Crystal packing of compound **5** is illustrated in Fig. 2. As can be seen from Fig. 2 crystal packing of compound **5** is dominantly arranged by a dense network of hydrogen bonds in a head-to-tail manner forming chains along the *b* axis. The hydrogen bond parameters are given in Table 2.

The X-ray structures of 3-hydroxy-secocyanoalcohol **1a** [14] and 3-hydroxy-16,17-seco-diol **5** were used as a basis for molecular docking studies. Docking studies were performed for protein targets of steroidal anti-cancer drugs: CYP17A1 (17αhydroxylase/17,20-lyase); CYP19A1 (aromatase); estrogen receptor (ERα) and

androgen receptor (AR). Note that molecular docking simulations were conducted against the active site of each protein, using grid maps centered on the coordinates of ligands in the respective protein structures. As a control, ligands present in X-ray structures of each protein were re-docked using the same grid maps and parameters. Control docking simulations accurately reproduced ligand–protein interaction geometries present in the respective X-ray structures. Predicted binding energies of compounds under study are presented in Table 3.

Molecular docking studies suggested strong binding of compounds **1**, **2**, **3** and **4** to lyase, compounds **2** and **4** to aromatase, and only compound **4** to estrogen receptor α and androgen receptor. The predicted binding of compound **2** to lyase was the strongest, even stronger then that predicted for the reference abiraterone, and stronger than binding of the same compound to aromatase (Fig. 3). Compound **4** non-selectively binds to all tested proteins with almost the same relative binding energies.
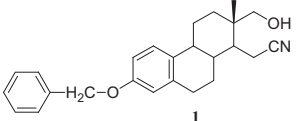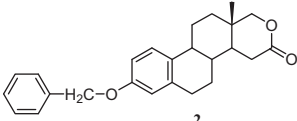
Table 2
Intramolecular O−H...O hydrogen-bond parameters (Å, °).

D−H...A	D−H	H...A	D...A	D−H...A
Compound 5				
O1−H1O...O2[1]	1.07(3)	1.64(4)	2.686(3)	165(3)
O2−H2O...O3	0.97(3)	1.81(3)	2.775(4)	174(3)
O3−H3O...O1[2]	1.01(3)	1.84(3)	2.814(4)	163(2)

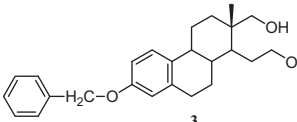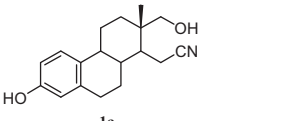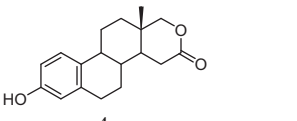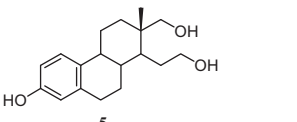[1] 1/2−x, 1−y, −1/2 + z.
[2] 1−x, 1/2 + y, 1/2−z.
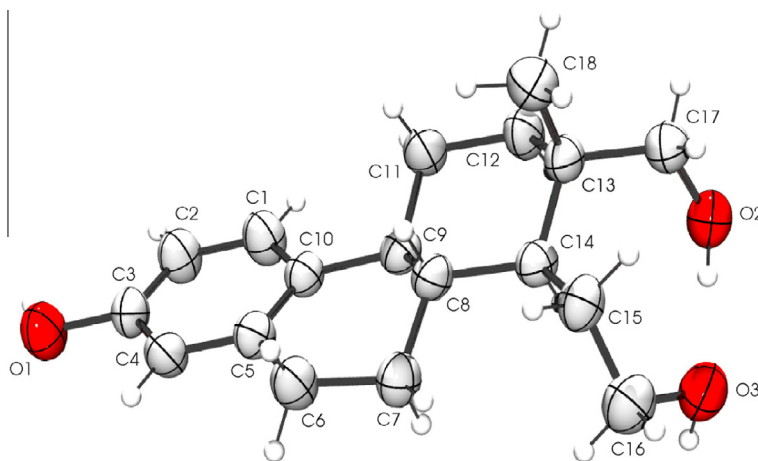
Fig. 1. ORTEP drawing of molecular structure of compound **5** with the labeling of non-H atoms. Displacement ellipsoids are shown at the 50% probability level and H atoms are drawn as spheres of arbitrary radii.
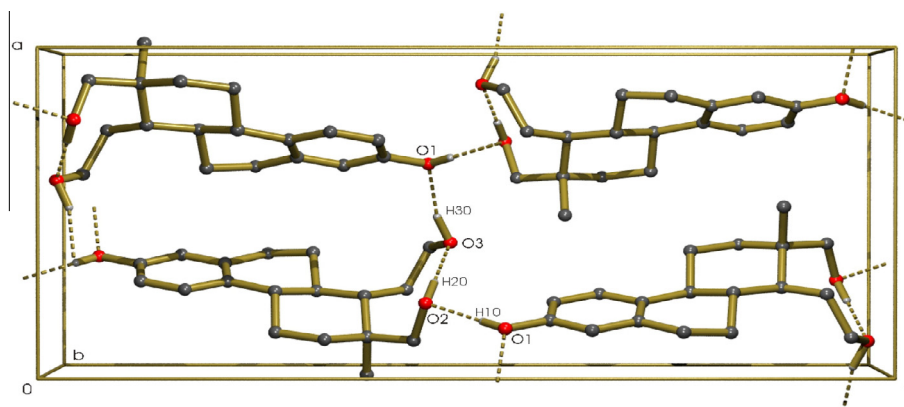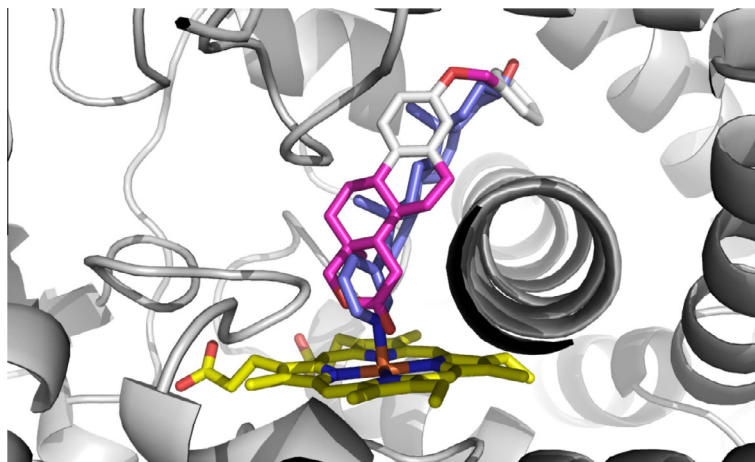

Fig. 2. PLATON drawing showing the crystal packing of compound **5**; Hydrogen bonds are shown as dashed lines.

Table 3
Predicted binding energies of compounds **1**, **1a** and **2–5** and reference compounds (calculated from molecular docking against known protein targets of steroidal anti-cancer drugs: CYP17A1 (17αhydroxylase/17, 20-lyase); CYP19A1 (aromatase); estrogen receptor (ERα) and androgen receptor (AR). Binding energies of ligands present in the X-ray crystal structure were calculated following re-docking.

Compound	Relative binding energy (Autodock, kcal/mol)			
	CYP17A1	CYP19A1	ERα	AR
1	−10.50	NB	NB	NB
2	−12.48	−11.01	NB	NB
3	−10.39	NB	NB	NB
1a	NB	NB	NB	NB
4	−10.17	−10.39	−10.10	−10.44
5	NB	NB	NB	NB
Abiraterone	−11.66	–	–	–
Androstenedione	–	−11.47	–	–
Estradiol	–	–	−10.26	–
Testosterone	–	–	–	−10.99

NB: no binding.

Fig. 3. Lyase docked with compound **2**. Docking energy−12.48 kJ/mol. Docking compound **2** (magenta) shows strong potential for coordination with the heme iron atom in 17,20 lyase, in a similar manner as abiraterone (blue).

Starting from these predictions of binding affinities, we performed biological tests, planning to measure the potential effects of the newly synthesised compounds *in vivo* and *in vitro*.

The estrogenic and antiestrogenic effects of compounds **2**, **3**, **4** and **5** were tested on experimental animals, using uterotropic and antiuterotropic methods [30], and compared with results

Table 4
Agonistic and antagonistic effects of compounds 1–5, 1a and tamoxifen.

Compound	Dose (mg/kg)	n	Estrogenic effect (%, mean ± SEM)	n	Antiestrogenic effect (%, mean ± SEM)
1	5	7	0.71 ± 0.90	8	31.47 ± 2.26
1a	5	6	−2.06 ± 1.06	8	21.13 ± 2.05
2	5	6	−2.61 ± 0.52	7	2.99 ± 3.81
3	5	6	−1.67 ± 1.38	7	−19.20 ± 9.47
4	5	6	−7.92 ± 1.96	8	20.93 ± 4.19
5	5	7	−8.49 ± 2.82	8	26.57 ± 5.38
Tamoxifen	5	7	39.78 ± 3.13	–	–
	25	8	39.36 ± 4.09	7	62.80 ± 2.13

Immature Wistar strain female rats (21–23 days old) were injected sc with 30 μg/kg b.w. (total dose) with the tested compounds **2–5** dissolved in olive oil (alone, or in combination with EB) or with vehicle alone (control) for 3 days. Number of animals per group was 6–8 (n). Results are presented as percentage of agonistic and antagonistic activity. Numbers represent mean ± SEM.

Table 5
Anti-aromatase and anti-lyase activity of the synthesised compounds 1, 1a and 2–5 and reference compounds aminoglutetimide and ketoconazole.

Compound	Concentration (μM)	Aromatase inhibition (%, mean ± SEM)	Lyase inhibition (%, mean ± SD)
1	50	–	NI
1a	50	–	36 ± 1
2	10	−14.81 ± 20,54	–
	50	26.71 ± 4.86	35 ± 6
3	10	−6.51 ± 21.44	–
	50	−23.02 ± 14.02	NI
4	10	1.50 ± 17.72	–
	50	−29.28 ± 9.0	17 ± 2
5	10	−39.36 ± 15.84*	–
	50	−34.52 ± 4.40*	14 ± 26
AG	0.1	41.33 ± 2.53**	–
Ketoconazole	–	–	IC_{50} = 0.32 ± 0.02 μM

Aromatase inhibition in denucleated fraction of ovaries from PMSG- pretreated rats: control group (10 probes), groups with tested compounds **2–5** and AG (4 probes for each). Results are presented as percentage of aromatase inhibition *vs.* control. Numbers represent mean ± SEM of 4 replicates. Significance (calculated for estradiol production): *$p < 0.05$; **$p < 0.005$ *vs.* control (Mann–Whitney non-parametric test); Lyase inhibition in the adult Wistar rat testicular tissue was performed in two experiments with each test compound and mean enzyme activity results with standard deviations were determined (mean ± SD). Results are presented as percentage of lyase inhibition *vs.* control. NI: no inhibition.
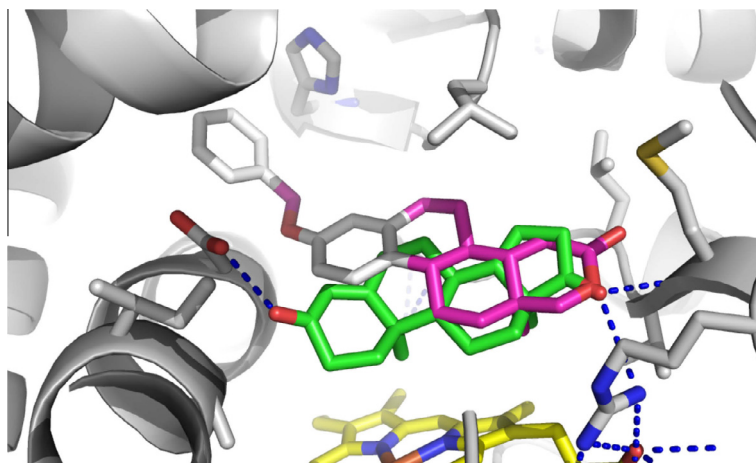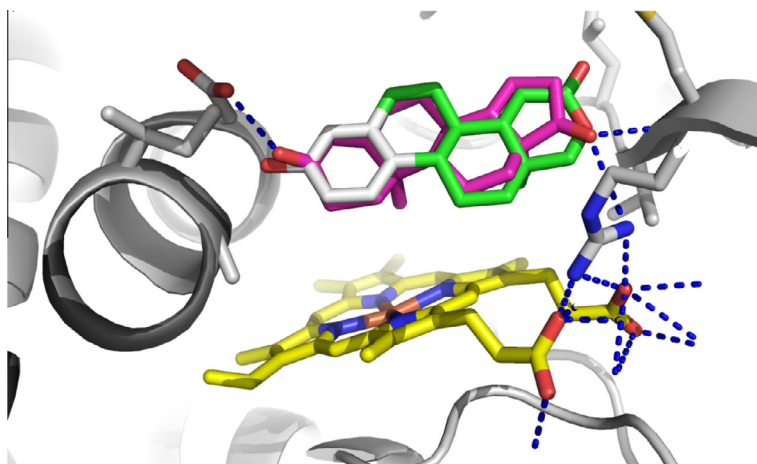

Fig. 4. Aromatase docked with compound **2**. Docking energy–11.01 kJ/mol. Docking compound 2 (magenta) shows similar hydrogen bonding potential as androstenedione green), with the aromatic ring substituent forming additional hydrophobic contacts, possibly explaining the high predicted binding affinity for this compound.

obtained before, for parent compounds, **1** and **1a** [11]. The differences of uteri weights of treated and control animals served for the calculation of the agonistic and antagonistic effects [31], presented in Table 4. Tamoxifen served in this experiment as positive control.

As can be seen from Table 4, compounds **4** and **5** (compounds with a free 3-hydroxy function) not only exhibited a total loss of estrogenic activity, but partially hindered the action of estradiol benzoate, behaving as moderate antagonists. 3-Benzyloxy D-homo

derivative **2** showed no hormonal or antihormonal activity, while 3-benzyloxy D-secoestratriene derivative **3** even enhanced estradiol benzoate activity.

Comparing the results of this experiment with results from earlier studies [11] (Table 4, compound **1** and its 3-hydroxy analog **1a**), we can see that compounds with a free C-3 hydroxy function (compounds **4** and **5**) were more potent antiestrogens, although the starting compound, secocyanoalcohol **1**, was more active than its 3-hydroxy derivative **1a**. Tamoxifen, the most used drug in

Fig. 5. Aromatase docked with compound **4**. Docking energy–10.39 kcal/mol. Androstenedione (magenta) is shown from crystal structure of aromatase. Note D-ring lactone forms hydrogen bonds similar to androstenedione. (For interpretation of the references to colour in this figure legend, the reader is referred to the web version of this article.)
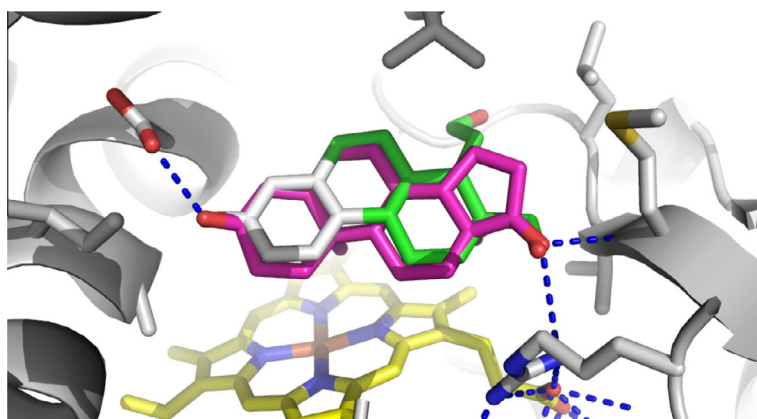
Fig. 6. Aromatase docked with compound **5**. Docking energy–9.6 kcal/mol. (intermolecular energy-11.39) Androstenedione (magenta) is shown from crystal structure of aromatase. Note D-seco enables hydrogen bond formation similar to androstenedione. (For interpretation of the references to colour in this figure legend, the reader is referred to the web version of this article.)

breast cancer therapy, showed higher antiestrogenic activity, but exhibited estrogenic potency also, which is consistent with its behavior as a partial estrogen.

An anti-aromatase assay was carried out for the purpose of screening the potential inhibitory effects of the newly synthesised compounds. The assay was conducted on the denucleated ovarian fraction from PMSG-pretreated female rats [32,33]. Estradiol production was measured in subsaturated concentrations of testosterone. The compounds were tested in two concentrations (10 μM and 50 μM). The results of the anti-aromatase assay are presented in Table 5. As can be seen, the newly synthesised compounds (except compound **2** at higher doses) activate aromatase. These results could be possibly utilized to guide the modeling and synthesis of therapeutics for the treatment of pathological conditions caused by estrogen depletion, e.g. osteopenia or osteoporosis. Predicted binding of selected new compounds with aromatase is presented in Figs. 4–6.

Table 5 includes the results of an anti-lyase assay as well. In the anti-lyase assay, compounds were tested at a concentration 50 μM where compounds **1a** and **2** were shown to be better lyase inhibitors than other compounds, but still not effective enough for therapeutic purposes.

Further derivatization of compounds tested are planned as follows: modification of **1** with the aim of obtaining compounds with higher antagonistic activity and modification of lactone **4**, which is predicted to bind strongly to all proteins under study.

Acknowledgements

Appendix A. Supplementary data

Supplementary data associated with this article can be found, in the online version, at http://dx.doi.org/10.1016/j.steroids.2014.08.026.

References

[1] Miller WL, Auchus RJ. The molecular biology, biochemistry, and physiology of human steroidogenesis and its disorders. Endocrine Reviews 2011;32(1):81–151.

[2] Hormone Therapy in Breast and Prostate Cancer. Jordan VC and Furr BJA, editors. New York: Springer; 2009.

[3] O'Donnell A, Judson I, Dowsett M, Raynaud F, Dearnaley D, Mason M, Harland S, Robbins A, Halbert G, Nutley B, Jarman M. Hormonal impact of the 17α-hydroxylase/C17,20-lyase inhibitor abiraterone acetate (CB7630) in patients with prostate cancer. British J Cancer 2004;90:2317–25.

[4] Avendano C, Menendez JC. Medicinal Chemistry of Anticancer Drugs. 1st ed. Oxford: Elsevier; 2008.

[5] Ghosh D, Griswold J, Erman M, Pangborn W. Structural basis for androgen specificity and oestrogen synthesis in human aromatase. Nature 2009;457:219–24.

[6] Miller WR, Larionov AA. Understanding the mechanisms of aromatase inhibitor resistance. Breast Cancer Res 2012;14:201–12.

[7] Smith IE, Dowsett M. Aromatase inhibitors in breast cancer. N Engl J Med 2003;348:2431–42.

[8] Aromatase Inhibitors. Furr JA., editor. 1st ed. Berlin: Barrington Birkhäuser Verlag; 2006.

[9] Bulin SE, Lin Z, Lin H, Imir G, Amin S, Demura M, Yilmaz B, Martin R, Utsunomiya H, Thung S, Gurates B, Tamura M, Langoi D, Deb S. Regulation of aromatase expression in estrogen responsive breast and uterine disease: from bench to treatment. Pharmacol Rev 2005;57:359–83.

[10] Santen RJ, Brodie H, Simpson ER, Siiteri PK, Brodie A. History of aromatase: saga of an important biological mediator and therapeutic target. Endocrine Reviews 2009;30(4):343–75.

[11] Jovanović-Šanta S, Andrić S, Kovačević R, Pejanović V. Synthesis and biological activity of new 16,17-secoestrone derivatives. Collect Czech Chem Commun 2000;65:77–82.

[12] Penov Gaši KM, Stanković SM, Csanadi JJ, Djurendić EA, Sakač MN, Medić Mijačević LJ, Arcson ON, Stojanović SZ, Andrić S, Molnar Gabor D, Kovačević R. New D-modified androstane derivatives as aromatase inhibitors. Steroids 2001;66:645–53.

[13] Penov-Gaši K, Stojanović S, Sakač M, Djurendić E, Jovanović-Šanta S, Stanković S, Andrić N, Popsavin M. Synthesis, crystal structure and antiaromatase activity of 17-halo-16,17-seko-5-androstene derivatives. J Serb Chem Soc 2003;68:707–14.

[14] Jovanović-Šanta S, Petrović J, Andrić S, Kovačević R, Đurendić E, Sakač M, Lazar D, Stanković S. Synthesis, structure, and screening of estrogenic and antiestrogenic activity of new 3,17-substituted -16,17-seco-estratriene derivatives. Bioorg Chem 2003;31:475–84.

[15] Penov-Gaši K, Stojanović SZ, Sakač MN, Popsavin M, Jovanović-Šanta S, Stanković SM, Klisurić OR, Andrić N, Kovačević R. Synthesis and anti-aromatase activity of some new steroidal D-lactones. Steroids 2005;70:47–53.

[16] Jovanović-Šanta S, Petrović J, Sakač M, Žakula Z, Isenović E, Ribarac-Stepić N. The influence of 17-oxo- and 17-hydroxy-16,17-seco-estratriene derivatives on estrogen receptor. Collect Czech Chem Commun 2006;71:532–42.

[17] Djurendić E, Daljev J, Sakač M, Čanadi J, Jovanović-Šanta S, Andrić S, Klisurić O, Kojić V, Bogdanović G, Djurendić-Bresnesel M, Novaković S, Penov-Gaši K. Synthesis of some epoxy and/or N-oxy 17-picolyl and 17-picolinylidene-androst-5-ene derivatives and evaluation of their biological activity. Steroids 2008;73:129–38.

[18] Jovanović-Šanta SS, Andrić S, Andrić N, Bogdanović G, Petrović JA. Evaluation of biological activity of new hemiesters of 17-hydroxy-16,17-secoestra-1,3,5(10)-triene-16-nitrile. Med Chem Res 2011;20:1102–10.

[19] Stoe, X-RED, Data Reduction for STADI4 and IPDS, Revision 1.08. Stoe & Cie, Darmstadt, 1996, Germany.

[20] Altomare A, Cascarano G, Giacovazzo C, Guagliardi A. Completion and refinement of crystal structures with SIR92. J Appl Cryst 1993;26:343–50.

[21] Farrugia LJ. WinGX suite for small-molecule single-crystal crystallography. J Appl Cryst 1999;32:837–8.

[22] Spek AL. PLATON. A Multipurpose Crystallographic Tool: University of Utrecht, The Netherlands; 1998.

[23] Sheldrick GM. SHELX97. Germany: Programs for Crystal Structure Analysis. University of Göttingrn; 1997.

[24] Nardelli MJ. PARST95 - an update to PARST: a system of Fortran routines for calculating molecular structure parameters from the results of crystal structure analyses. J Appl Cryst 1995;28:659–62.

[25] Pedretti A, Villa L, Vistoli GJ. Comput Aided Mol Des 2004;18:167–73.

[26] Hanwell MD, Curtis DE, Lonie DC, Vandermeersch T, Zurek E, Hutchison GRJ. Avogadro: an advanced semantic chemical editor, visualization, and analysis platform Cheminform, 2012; 4:17–34.

[27] Morris GM, Huey R, Lindstrom W, Sanner MF, Belew RK, Goodsell DS, Olson AJ. AutoDock4 and AutoDockTools4: automated docking with selective receptor flexibility. J Comput Chem 2009;30:2785–91.

[28] Ren J, Williams N, Clementi L, Krishnan S, Li WW. Opal web services for biomedical applications. Nucleic Acids Res 2010;38:W724–31.

[29] Wolf LK. New software and websites for the chemical enterprise. Chem Eng News 2009;87:31–47.

[30] Emmens CW. Hormone assay. New York: Academic Press; 1950.

[31] Wakeling AE, Valcaccia B, Newboult E, Green LR. Non-steroidal anti-oestrogens-receptor binding and biological response in rat uterus, rat mammary carcinoma and human breast cancer cells. J Steroid Biochem 1984;20:111–20.

[32] Brodie AMJ, Schwarzel WC, Brodie HJ. Studies on the mechanism of estrogen biosynthesis in the rat ovary. J Steroid Biochem 1976;7:787–93.

[33] Iványi Z, Szabó N, Huber J, Wölfling J, Zupkó I, Szécsi M, Wittmann T. Schneider Gy. Synthesis of D-ring-substituted (5' R)- and (5' S)-17α-pyrazolinylandrostene epimers and comparison of their potential anticancer activities. Steroids 2012;77:566–74.

[34] Kovács D, Wölfling J, Szabó N, Szécsi M, Kovács I, Zupkó I, Frank É. An efficient approach to novel 17–5'-(1',2',4')-oxadiazolyl androstenes via the cyclodehydration of cytotoxic O-steroidacylamidoximes, and an evaluation of their inhibitory action on 17α-hydroxylase-C17,20-lyase. Eur J Med Chem 2013;70:649–60.